Astron. Nachr. / AN **333**, No. 4, 319 – 323 (2012) / **DOI** 10.1002/asna.201211664

Suzaku observations of charge exchange emission from solar system objects

Y. Ezoe[1,⋆], **R. Fujimoto**[2], **N.Y. Yamasaki**[3], **K. Mitsuda**[3], **T. Ohashi**[1], **K. Ishikawa**[1], **S. Oishi**[1], **Y. Miyoshi**[4], **N. Terada**[5], **Y. Futaana**[6], **F.S. Porter**[7], and **G.V. Brown**[8]

[1] Tokyo Metropolitan University, 1-1 Minami-Osawa Hachioji, Tokyo 192-0397, Japan
[2] Kanazawa University, Kakuma-chou, Kanazawa, Ishikawa 920-1192, Japan
[3] The Institute of Space and Astronautical Science, 3-1-1 Yoshinodai, Tyuou-ku, Sagamihara, Kanagawa 252-5210, Japan
[4] Nagoya University, Furo-cho, Chikusa-ku, Nagoya 464-8601, Japan
[5] Tohoku University, 6-3 Aoba, Aramaki, Aoba-ku, Sendai, Miyagi 980-8578, Japan
[6] Swedish Institute of Space Physics, Box 812, SE-98128 Kiruna, Sweden
[7] NASA/Goddard Space Flight Center, Greenbelt, MD 20771, USA
[8] Lawrence Livermore National Laboratory, 7000 East Avenue L-260 Livermore, CA 94550, USA

Received 2012 Mar 2, accepted 2012 Mar 8
Published online 2012 Apr 20

Key words comets: individual (73P/SW3 fragment C) – Earth – planets and satellites: individual (Jupiter, Mars) – solar-terrestrial relations – solar wind

Recent results of charge exchange emission from solar system objects observed with the Japanese Suzaku satellite are reviewed. Suzaku is of great importance to investigate diffuse X-ray emission like the charge exchange from planetary exospheres and comets. The Suzaku studies of Earth's exosphere, Martian exosphere, Jupiter's aurorae, and comets are overviewed.

1 Introduction

Recent X-ray observations have revealed that the charge exchange process produces X-ray emission in various solar system environments such as comets, planetary exospheres, aurorae, and the heliosphere (see Bhardwaj et al. 2007 for a review). When an ion in the solar wind or planetary magnetosphere interacts with a neutral atom, it strips an electron(s) from the atom, and releases X-ray photon(s) as the the captured electron relaxes into the ground state. The charge exchange emission is thus characterized by a sum of emission lines and can, in some cases, be distinguished from ordinary thin thermal plasma emission by strong lines from large principle quantum number states and forbidden lines (Krasnopolsky, Greenwood & Stancil 2004).

Charge exchange emission is now recognized to be important for not only astrophysics but also for magnetospheric and atmospheric physics. It can provide valuable information on the density of the tenuous atmosphere of planets and comets, the shape of the magnetosphere, and the transportation of the solar wind ions and accelerated ions in the magnetosphere. Not only observational but also theoretical studies have been pursued to predict the solar wind charge exchange (SWCX) in Earth's exosphere (Robertson & Cravens 2002; Snowden et al. 2009), a comet (Lisse et al. 2005) and the heliosphere (Koutroumpa et al. 2006)

The Japanese Suzaku satellite is very useful in understanding charge exchange X-ray emission because of the good energy response and low instrument background of its X-ray CCDs (XIS: X-ray Imaging Spectrometer). A review of the solar system planets observed with Suzaku has been described in Ezoe et al. (2011a). In this paper, we review recent studies of the charge exchange emission from solar system objects with Suzaku.

2 Earth

SWCX emission in Earth's exosphere can constitute an additional source of background in astrophysical observations. This emission was found during the ROSAT all-sky survey as long term enhancements (Snowden et al. 1994). A systematic study for the exospheric SWCX in the XMM-Newton archival data by Carter, Sembay and Read (2011) identified that about 3 % of the sample is contaminated by the temporally variable SWCX. This unwanted background for general users of X-ray astronomical satellites can be a new tool to study the solar wind and Earth's exosphere. Since the SWCX emission is expected to be proportional to the solar wind flux and exospheric column density, the combination of X-ray and solar wind data allows quantitative estimation of the exospheric density. If high enough photon statistics data are available, examination of the time delay between the X-ray light curve and solar wind curve

⋆ Corresponding author: ezoe@tmu.ac.jp

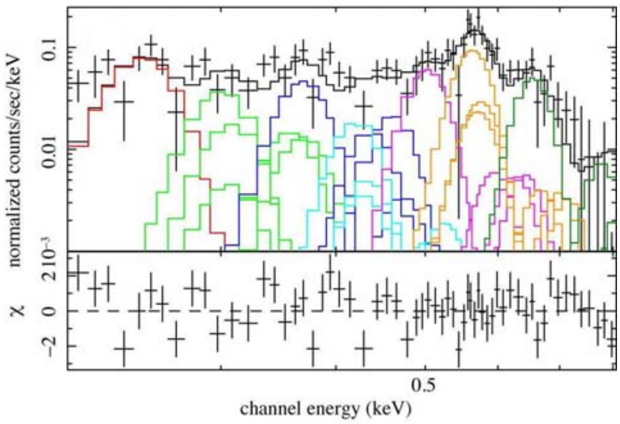

Fig. 1 (online colour at: www.an-journal.org) XIS spectrum during the strong geomagnetic storm recorded on 2005 August 24 (Ezoe et al. 2011b). The lines due to C, N, and O are color coded: C V (green), C VI (blue), N VI (cyan), N VII (magenta), O VII (orange), and O VIII (dark green).

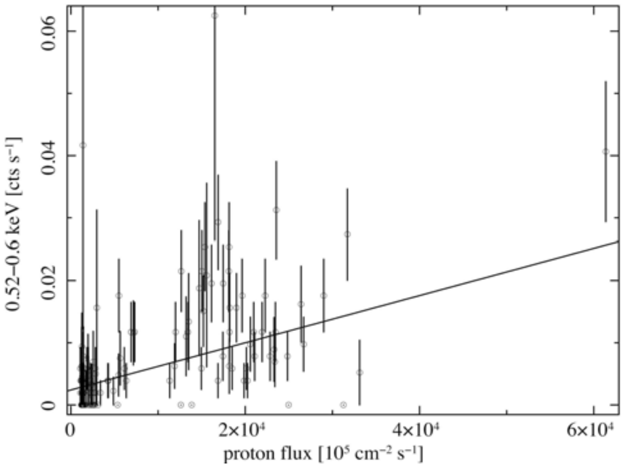

Fig. 2 Correlation between the XIS O VII count rate and the WIND proton flux during the strong geomagnetic storm (Ezoe et al. 2011b). The solid curve is the best-fit linear function.

can constrain the transportation of the solar wind in the interplanetary space and possibly magnetosphere.

Fujimoto et al. (2007) detected increases of emission lines such as C VI 4p–1s during the observation of the north ecliptic pole region (a blank sky background observation) taken in 2005 September shortly after launch (2005 July). A good time correlation with the increased solar wind proton flux and the strength of the emission line support the view that it originates as SWCX emission in Earth's exosphere. Since the line of sight direction was toward the magnetic pole, the emission should arise near a cusp of the Earth's magnetosphere where the solar wind penetrates to as low as $\sim$2 Earth radii.

Ezoe et al. (2010a) found a temporally variable OVII line in a deep observation of galactic ridge emission in 2005 October. The line flux was too strong to originate inside the heavily obscured galactic disk. A good time correlation with the solar wind proton and O ion data taken by the ACE satellite was observed. The time delay estimated from the cross correlation analysis was consistent with the travel time of the solar wind from ACE to Suzaku ($\sim$1 hr). Thus, this emission should arise from the charge exchange. However, there remained an issue on the exospheric column density. In this observation, the line of sight direction was toward the flank of the magnetosheath. The expected line intensity based on the exospheric density model and the solar wind flux was at least $\sim$10 times smaller than the observation because the closest distance at which the solar wind can interact with the exospheric neutrals should be large, $\sim$10 Earth radii, and hence the column density of the exospheric neutrals becomes small. Since this estimation is based on simple assumptions in terms of the exospheric density and solar wind distribution, a full treatment of the magnetohydrodynamics of the solar wind flow into the magnetosheath and the interaction with a more complete model for exospheric hydrogen is needed.

Motivated by these results, Ezoe et al. (2011b) searched Suzaku data for time variable charge exchange emission, focusing on a strong geomagnetic storm occurred on 2005 August 24. The Dst index, an indicator of the geomagnetic storm, was -216 nT, the strongest that Suzaku has experienced (to 2012 February). Enhanced emission lines from ionized C, N, and O were successfully detected in the corresponding Suzaku data. Strong line intensities and time variability supports the SWCX emission scenario. The spectrum during the charge exchange enhancement was well represented by the SWCX model constructed by Bodewits (2007) as shown in Fig. 1. Also, the time delay estimated in the same way as Ezoe et al. (2010a) was consistent with the SWCX interpretation. Figure 2 shows the correlation between the Suzaku O VII count rate and the solar wind proton flux where the time delay has been included. The proportionality coefficient represents the SWCX emissivity, while the ordinate intercept is an offset emission due to the sky and instrumental background. This plot has an advantage over the simple comparison of the X-ray intensity and solar wind flux averaged over the observational duration, because the background can be distinguished from the fitting and the theoretically predicted linear relation can be directly examined. To investigate anisotropy of the SWCX emissivity depending on the line of sight direction, the authors are applying this analysis to other Suzaku archival data.

3 Mars

Similar to Earth, the SWCX emission in the Martian exosphere has been detected as halo emission extended over several Martian radii with Chandra (Dennerl 2002). A high resolution spectrum obtained with XMM-Newton showed signs of emission lines from highly ionized C, N, O and Ne atoms and a CO_2 molecule (Dennerl et al. 2006). The high photon-statistics XMM-Newton image also revealed that the emission from ionized O may flow out from the

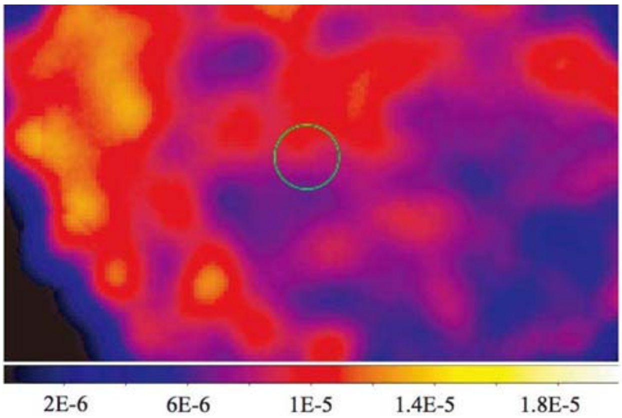

Fig. 3 (online colour at: www.an-journal.org) XIS image after a correction for the orbital motion of Suzaku and Mars's ephemeris in 0.2–1 keV (Ishikawa et al. 2011). A circle indicate the expected position of Mars. Its diameter of 2 arcmin considers the half power diameter of Suzaku and pointing accuracy.

Martian poles to the antisolar direction. These results are strong lines of evidence that the escaping exospheric neutrals from Mars interact with the solar wind ion and emit the charge exchange X-rays. Therefore, X-ray observations of the SWCX in the Martian exosphere can be a probe to study the exospheric neutral atoms of Mars.

Ishikawa et al. (2011) observed Mars with Suzaku for the first time at solar minimum in X-rays in 2008 April. The past Chandra and XMM-Newton observations were conducted at solar maximum in 2001 July and 2003 November, respectively. Among exospheric density models based on measurements by exploration missions (e.g., Anderson 1974), some models (e.g., Krasnopolsky 2002) imply a high dependence on the solar cycle. Therefore, this observation provides us with a good opportunity to investigate a potential change of the exospheric SWCX.

The 0.2–1 keV image after a correction for the orbital motions of Suzaku and Mars's ephemeris is shown in Fig. 3. No significant X-ray photons were detected at the position of Mars. Figure 4 shows the X-ray spectra of Mars compared to the surrounding background. A 2σ upper limit of the Martian X-ray emission was 4.3×10^{-5} photons $\mathrm{cm}^{-2}\,\mathrm{s}^{-1}$ in the O VII line band (0.5–0.65 keV). The upper limit of the exospheric neutral density during the Suzaku observation was placed considering the solar wind proton flux, the geocentric and heliocentric distances. The implied Martian exospheric densities inferred by the Suzaku observations are factors of $\sim$70 and $\sim$6 lower than during the Chandra and XMM-Newton observations, respectively. Although this result can not completely reject the higher exospheric density at lower solar activity, the change of the exospheric density was for the first time constrained from the X-ray data.

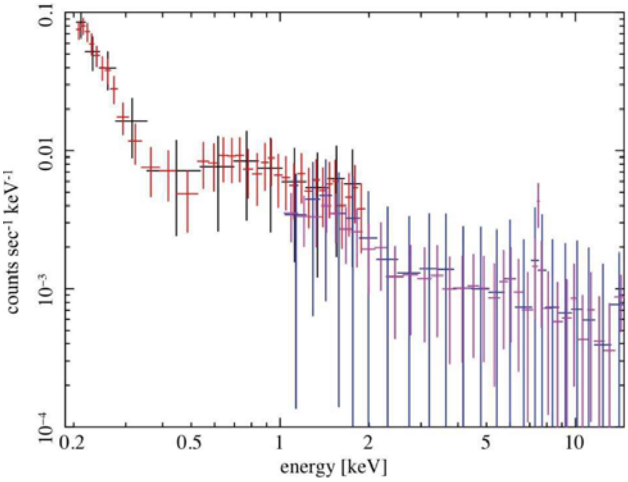

Fig. 4 (online colour at: www.an-journal.org) XIS spectra of Mars compared to the background (Ishikawa et al. 2011). The back-illuminated CCD spectra are shown in black (Mars) and red (background), while the front-illuminated spectra are in blue (Mars) and magenta (background).

4 Jupiter

Jupiter's X-ray emission has been known since the 1980's (Metzger et al. 1983). It can be classified into two types (Gladstone et al. 2002; Branduardi-Raymont et al. 2004). One is the low latitude disk emission due to solar X-rays scattered by the upper atmosphere. The other is the auroral emission composed of electron bremsstrahlung continuum and emission lines with high charge states of O, and C (and/or S). High resolution spectra obtained with XMM-Newton in the range of 0.5–1 keV clearly separated O VII and O VIII emission lines, which seemed to possess broad wings. Implied velocities of $\sim$5000 $\mathrm{km\,s^{-1}}$ are consistent with the scenario that high energy ions accelerated in the magnetosphere to several MeV strip an electron(s) from neutrals in the upper atmosphere and emit X-rays via the charge exchange process. There are two candidates for the origin of the precipitating ions. One is Jupiter's inner magnetosphere, where an abundance of S and O atoms associated with Io and its plasma torus can be expected. The other possible source is the solar wind in which an abundance of C will be dominant for the emission line around 0.3 keV.

Suzaku observed Jupiter in 2006 February and detected significant X-ray emission (Ezoe et al. 2010b). Figure 5 shows the X-ray images of Jupiter. In the 0.2–1 keV band, a point-like X-ray source was detected at the position of Jupiter, while, in 2–5 keV, a diffuse X-ray emission was seen. The X-ray spectrum of the diffuse X-ray emission shown in Fig. 6 was represented by a sum of a power law and two Gaussian lines. The photon index of the power law was $\sim$1.4. Considering the extended feature and the hard power law continuum, Ezoe et al. (2010b) suggested that the origin of the emission could be inverse Compton scattering of solar photons by tens of MeV electrons in the inner radiation belts. The soft X-ray emission was dominated by

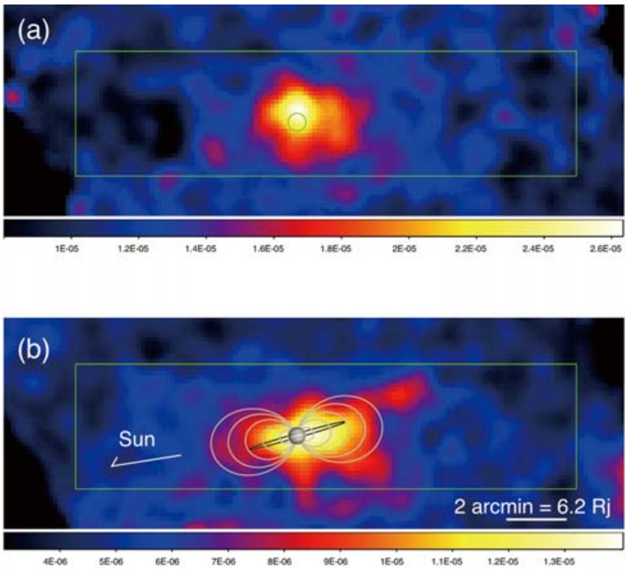

Fig. 5 (online colour at: www.an-journal.org) XIS images after correcting for the satellite's orbital motion and Jupiter's ephemeris in the (*a*) 0.2–1 keV and (*b*) 2–5 keV bands (Ezoe et al. 2010b). A circle indicates the expected position and size of Jupiter. Grey lines indicate the equatorial crossing of magnetic field lines. A black line is the path traced by Io. A photograph of Jupiter by Cassini is overlaid in the panel (*b*).

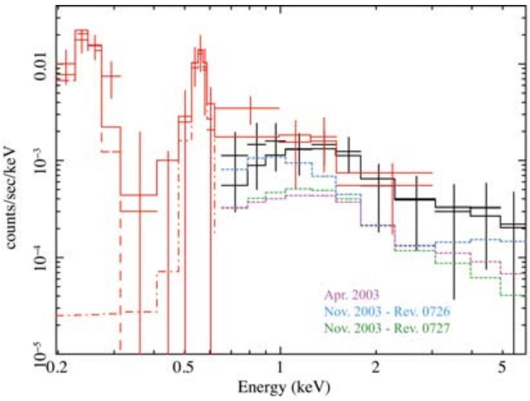

Fig. 6 (online colour at: www.an-journal.org) Background subtracted XIS spectrum of the diffuse emission region, compared with the best-fit power-law plus two Gaussian models (solid line). Dashed lines are Jupiter's auroral continuum emission models in XMM-Newton observations.

the two Gaussians, whose center energies were $\sim$0.24 and $\sim$0.56 keV. These are presumably a line complex from C VI and ionized Mg, Si, S, and O VII Kα emission, respectively. Taken together with the fact that the 0.2–1 keV X-rays arise from a point-like source, most of soft X-rays likely originate from Jupiter's aurora via charge exchange, although the exact origin of the ion source is still unclear because of the limited energy resolution of the X-ray CCDs.

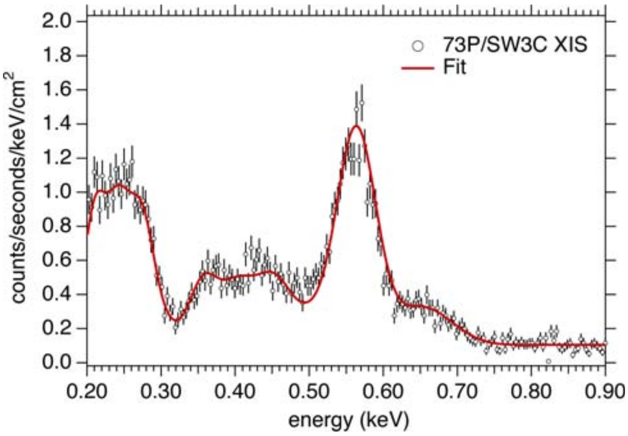

Fig. 7 (online colour at: www.an-journal.org) Background subtracted XIS spectrum of the comet 73P/SW3 fragment C measured on 2006 June 8 (Brown et al. 2009). A solid line indicates the laboratory measured charge exchange spectral model composed of C V, C VI, N VI, N VII, and O VII. Additional lines at 0.21, 0.24, 0.27, and 0.4 keV are included.

5 Comets

Comets are prototypical SWCX sources (Lisse et al. 1996). The number density of the widely extended (10^{4-6} km in size) cometary coma ranges 10^{0-8} molecules cm^{-3} depending on the distance from the core of the coma (e.g., Lisse et al. 2005). This tenuous and extended coma is a very efficient source of charge exchange with the total amount of energy emitted in X-rays being 10^{-4} to $\sim 10^{-5}$ of the optical wavelength range (Lisse et al. 2004). This efficiency is about 10^5 times larger than those of solar system objects (Ezoe et al. 2011a). Since the comets are one of the brightest X-ray sources in the solar system, the study of the cometary X-ray emission can lead us to a better understanding of the nature of the cometary coma, the properties of the solar wind, and the SWCX process which is known to play an important role in other astrophysical objects.

Suzaku observed the 73P/SW3 fragment C on 2006 May 13 at its closest approach to Earth at a distance of 0.074 AU and again at perihelion on 2006 June 8 (Brown et al. 2009). On the latter observation, a corotational interaction region of the solar wind hit the comet and the X-ray emission from the comet brightened. Figure 7 shows the X-ray spectrum measured on June 8. The data were well fitted with a laboratory measured charge exchange model composed of highly ionized C, N, and O lines. In addition, lines at the low energy band less than 0.4 keV were included to better represent the data. Many of these lines are most likely produced by charge exchange onto L-shell ions of Si, S, and Mg. As a diagnostic tool of the solar wind speed, the hardness ratio defined as relative intensity of the principal quantum number state $n > 3$ to 1 transitions relative to the $n = 2$ to 1 transitions was used. When the larger hardness ratio is larger, the speed of the solar wind ion relative to the cometary neutral becomes slower (Beisersdorfer et al. 2001). The estimated velocity of the C VII ions is $\sim$300 km s^{-1}, consistent with a slow solar wind.

6 Summary and future

With the good energy response and the low instrument background of the Suzaku X-ray CCDs, our understanding of the charge exchange emission from solar system objects (Earth's exosphere, Martian exosphere, Jupiter's aurorae, and comets) is being advanced with Suzaku. Comprehensive studies of the SWCX in the Earth's exosphere and the heliosphere are undergoing.

In 2014, Astro-H will launch carrying a high resolution X-ray microcalorimeter array. This instrument will have an order of magnitude better energy resolution of 7 eV (or better) than X-ray CCDs. The large effective area of 200 cm^2 at 1 keV will enable progress in understanding the charge exchange emission of diffuse sources like planetary exospheres and comets. Emission lines from highly ionized ions such as C, S, N, and O can be resolved. The chemical composition, the origin in the case of Jupiter, and the speed of the input ions can be determined. Not only the ions but also the species of the target neutral atoms and molecules will be able to be distinguished from the spectral distribution of the emission lines as demonstrated by Beisersdorfer et al. (2003) using the spare detector of the Astro-E satellite mission.

Acknowledgements. Work by LLNL was completed under Contract DE-AC52-07NA27344.

References

Anderson, D.E., Jr.: 1974, J. Geophys. Res. 79, 1513
Beisersdorfer, P., et al.: 2001, AJ 549, L147
Beisersdorfer, P., et al.: 2003, Sci 300, 1558
Bhardwaj, A., et al.: 2007, Planetary Space Sci. 55, 1135
Bodewits, D.: 2007, PhD Thesis, University of Groningen
Branduardi-Raymont, G.: 2004, A&A 424, 331
Brown, G.V., et al.: 2009, in: *The Energetic Cosmos: from Suzaku to Astro-H*, p. 190
Carter, J.A., Sembay, S., Read, A.M.: 2011, A&A 489, 837
Dennerl, K.: 2002, A&A 394, 1119
Dennerl, K., et al.: 2006, A&A 451, 709
Ezoe, Y., et al.: 2010a, PASJ 62, 981
Ezoe, Y., et al.: 2010b, AJ 709, L178
Ezoe, Y., et al.: 2011a, Adv. Space Res. 47, 411
Ezoe, Y., et al.: 2011b, PASJ 63, 691
Fujimoto, R., et al.: 2007, PASJ 59, S133
Gladstone, G.R.: 2002, Nature 415, 1000
Ishikawa, K., et al.: 2011, PASJ 63, 705
Koutroumpa, D., et al.: 2006, A&A 460, 289
Krasnopolsky, V.A.: 2002, J. Geophys. Res. 73, 7149
Krasnopolsky, V.A., Greenwood, J.B., Stancil, P.C.: 2004, Space Sci. Rev. 113, 271.
Lisse, C.M., et al.: 1996, Sci 274, 205
Lisse, C.M., et al.: 1996, AJ 635, 1329
Lisse, C.M., Cravens, T.E., Dennerl, K.: 2004, in: M.C. Festou, H.U. Keller, H.A. Weaver (eds.), *Comets II*, p. 631
Lisse, C.M., et al.: 2005, ApJ 635, 1329
Metzger, A.E., et al.: 1983, J. Geophys. Res. 83, 7731
Robertson, I.P., Cravens, T.E.: 2002, Geophys. Res. Lett. 30, 1439
Snowden, S.L., et al.: 1994, AJ 424, 714
Snowden, S.L., et al.: 2009, AJ 691, 372